Available online at www.sciencedirect.com
ScienceDirect
Biochimica et Biophysica Acta 1758 (2006) 1359–1372
BIOCHIMICA ET BIOPHYSICA ACTA
BBA
www.elsevier.com/locate/bbamem

Investigating molecular recognition and biological function at interfaces using piscidins, antimicrobial peptides from fish

Eduard Y. Chekmenev [a], Breanna S. Vollmar [b,c], Kristen T. Forseth [b,c], McKenna N. Manion [b,c], Shiela M. Jones [b], Tim J. Wagner [b], RaeLynn M. Endicott [c], Brandon P. Kyriss [c], Lorraine M. Homem [c], Michelle Pate [d], Jing He [d], Joshua Raines [d], Peter L. Gor'kov [a], William W. Brey [a], Dan J. Mitchell [e], Ann J. Auman [c], Mary J. Ellard-Ivey [c], Jack Blazyk [d], Myriam Cotten [b,*]

[a] *National High Magnetic Field Laboratory, Center for Interdisciplinary Magnetic Resonance, 1800 E. Paul Dirac Drive, Tallahassee, FL 32310, USA*
[b] *Department of Chemistry, Pacific Lutheran University, 1010 122d Street South, Tacoma, WA 98447, USA*
[c] *Department of Biology, Pacific Lutheran University, 1010 122d Street South, Tacoma, WA 98447, USA*
[d] *Department of Biomedical Sciences, College of Osteopathic Medicine, and Department of Chemistry and Biochemistry, College of Arts and Sciences, Ohio University, Athens, OH 45701, USA*
[e] *Department of Biochemistry and Biophysics, Washington State University, Pullman, Washington 99163-4660, USA*

Received 26 December 2005; received in revised form 26 March 2006; accepted 31 March 2006
Available online 7 April 2006

Abstract

We studied amidated and non-amidated piscidins 1 and 3, amphipathic cationic antimicrobial peptides from fish, to characterize functional and structural similarities and differences between these peptides and better understand the structural motifs involved in biological activity and functional diversity among amidated and non-amidated isoforms. Antimicrobial and hemolytic assays were carried out to assess their potency and toxicity, respectively. Site-specific high-resolution solid-state NMR orientational restraints were obtained from ^{15}N-labeled amidated and non-amidated piscidins 1 and 3 in the presence of hydrated oriented lipid bilayers. Solid-state NMR and circular dichroism results indicate that the peptides are α-helical and oriented parallel to the membrane surface. This orientation was expected since peptide–lipid interactions are enhanced at the water–bilayer interface for amphipathic cationic antimicrobial peptides. ^{15}N solid-state NMR performed on oriented samples demonstrate that piscidin experiences fast, large amplitude backbone motions around an axis parallel to the bilayer normal. Under the conditions tested here, piscidin 1 was confirmed to be more antimicrobially potent than piscidin 3 and antimicrobial activity was not affected by amidation. In light of functional and structural similarities between piscidins 1 and 3, we propose that their topology and fast dynamics are related to their mechanism of action.

Keywords: Piscidin; Structure–function relationship; Solid-state NMR; Oriented lipid bilayer; Peptide dynamics; Water–bilayer interface

Abbreviations: ACAPs, antimicrobial, cationic, amphipathic peptides; CD, circular dichroism; DPG, diphosphatidylglycerate; DMPC, 1,2-dimyristoyl-*sn*-glycero-3-phosphocholine; DMPG, 1,2-dimyristoyl-*sn*-glycero-3-phosphoglycerate; DTPC, 1,2-*O*-ditetradecyl-*sn*-glycero-3-phosphocholine; DTPG, 1,2-*O*-ditetradecyl-*sn*-glycero-3-phosphoglycerate; HPLC, high performance liquid chromatography; LPS:, lipopolysaccharides; LUVs, large unilamellar vesicles; MIC, minimal inhibitory concentration; NMR, nuclear magnetic resonance; p1(or 3)-COO^-, non-amidated piscidin 1 (or 3); p1(or 3)-NH_2, amidated piscidin 1 (or 3); PC, phosphatidylcholine; PDB, protein data bank; PE, phosphatidylethanolamine; PISEMA, Polarization Inversion Spin Exchange at the Magic Angle; PG, phosphatidylglycerol; POPC, 1-palmitoyl-2-oleoyl-*sn*-glycero-3-phosphatidylcholine; POPG, 1-palmitoyl-2-oleoyl-*sn*-glycero-3-phosphatidylglycerate; REDOR, Rotational Echo DOuble Resonance; TFE, trifluoroethanol; UV, ultraviolet

* Corresponding author. Tel.: +1 253 535 7555; fax: +1 253 536 5055.
E-mail address: cottenml@plu.edu (M. Cotten).

0005-2736/$ - see front matter © 2006 Elsevier B.V. All rights reserved.
doi:10.1016/j.bbamem.2006.03.034

1. Introduction

Piscidins or moronecidins, co-discovered by Silphaduang and Noga [1] and Lauth et al. [2] in hybrid striped bass (*Morone saxatilis* x *M. chrysops*), are the first antimicrobial amphipathic cationic peptides (ACAPs) ever found in the mast cells of animals. Piscidins 1 and 2, which are also known as sb-moronecidin and wb-moronecidin, respectively, were also found in each parental stock of hybrid striped bass. Present in the skin, gills and gastrointestinal tract of this fish, piscidins 1, 2, and 3 are believed to play a crucial, direct role in the fight against many aquatic bacterial infections. Antimicrobial peptides as part of innate immunity represent an important mechanism of defense in fish and other vertebrates with primitive immune systems [3–7]. Since fish have been considered as a source of natural antibiotics only recently, there have been few reports of antimicrobial peptides from fish [7,8]. Other antimicrobial peptides originating from fish include chrysophsin [9], bass hepcidin [10], hipposin [11], misgurin [12], pleurocidin [13,14], and pardaxin [15]. Piscidins have broad-spectrum activity against antibiotic-resistant bacteria filamentous fungi, yeast, and viruses [1,2,16]. Interestingly, piscidins 1, 2, and 3, each 22-amino acid long, are characterized by several special features [1,2,7]. Piscidins have highly conserved amino ends featuring several isoleucines, phenylalanines, and histidines. Piscidins may exist in a carboxyamidated form. While it is not unusual for ACAPs to be amidated, piscidins were reported to be the first amidated ACAPs isolated from fish. The biological significance of this modification is not fully understood. Piscidins are tolerant to high salt concentrations. Piscidin 2, which differs from piscidin 1 only at position 18 (R in piscidin 1 vs. K in piscidin 2), was found to be still active against *S. aureus* at sodium chloride concentrations up to 1280 μM [2]. In a comparative analysis among a few antimicrobial peptides done by Noga and Silphaduang [7] in 2003, piscidin 2 performed as the most salt-tolerant peptide with respect to monovalent and divalent cations. In terms of charge, arginine and lysine contribute to the high cationic character and pI of piscidins (e.g., pI of 12.4 for piscidin 1). Finally, piscidins have a high content of histidine, i.e., four in piscidins 1 and 2, and three in piscidins 3.

Detailed characterization of piscidin structure is a necessary step in the search for relationships between structural motifs, interactions with biological membranes, potency, and mechanisms of action. Many recent studies of ACAPs have produced a large amount of information, which can be used to facilitate the structural study of piscidins. ACAPs vary greatly in terms of amino acid content, length, ability to interact with membranes, and effects of pH and salt concentrations on antimicrobial activity. Minimal Inhibitory Concentrations (MICs) vary greatly, as well [3–5,17–23]. A large number of cationic antimicrobial peptides can interact, at least initially, with negatively-charged microbial membranes, which suggests that molecular interactions at the water–bilayer interface are important for target recognition [24–31]. Furthermore, bilayer composition can affect the peptide depth of penetration and ability to impact lipid organization and dynamics. ACAPs' amphipathic structures, molecular volumes, and aggregation states in solution and the membrane have been considered important for function [30–34]. In an aqueous medium, ACAPs are unstructured, but they usually become structured in the presence of lipid bilayers and organic solvents. Out of the five major structural classes described for ACAPs, α-helices (e.g., cecropins, magainin) and β-sheets (e.g., defensins, protegrin-1, tachyplesin) dominate [17,20,22,30–37]. 3-D structures of ACAPs in the Protein Data Bank (PDB) feature a number of α-helical and β-sheet antimicrobial peptides [33]. The fact that, in the presence of bilayers, ACAPs adopt amphipathic structures hints at the importance of secondary structure for optimized recognition and interactions with targets. Hence amphipathic structures seem to optimize electrostatic and/or hydrophobic interactions between the peptides and their environment. While the interactions with microbial membranes, the membrane permeation effect, and the formation of channels have been documented for many ACAPs [6,17,20,22,24,25,27,30–37], there is still a question about whether they kill bacteria due to cell lysis concomitant with bilayer disruption and/or channel formation or whether they translocate inside the cell where they bind anionic targets and activate pathways leading to cell death [17,22,30–38]. Thus, fully understanding how ACAPs work may involve studying the possible synergy between several functions ("multihit" mechanism involving multiple negatively-charged targets including intracellular DNA) as well as realizing that the diversity in amino acid sequences and structures may translate in a variety of mechanisms of action. Mechanisms of action currently discussed [17,22,30–38] include: (1) the barrel-stave model with transmembrane pore formation, possibly voltage-dependent; (2) the wormhole model with formation of peptide–lipid association in "torodial pores"; (3) the "carpet" mechanism with a monolayer distribution of peptide; (4) in plane-diffusion, which does not require self-association. The permeation effect caused by the formation of pores seems to include peptide binding to the membrane prior to formation of a co-assembly leading to permeation at a threshold concentration. "Detergent-like" or micellization effects and "sinking rafts" of peptides making their way across membranes represent other possible mechanisms of action [37,38]. Hancock et al. [39] have suggested that ACAPs cross the membrane of gram-negative bacteria using a "self promoted uptake" mechanism which includes charge-mediated binding of ACAPs to lipopolysaccharides (LPS) followed by crossing of the outer of membrane to reach the inner membrane, where lethal activity can be initiated.

Due to their amphipathic structures, ACAPs whose bilayer location is known prefer binding on the bilayer surface, but some ACAPs may adopt a transmembrane orientation. In fact, some ACAPs can have in-plane and/or transmembrane orientations depending on the environment conditions. Examples include melittin [40,41], pardaxin [42], and synthetic LAH4 [43]. Aromatic amino acids are often found at interfaces [44,45] where they seem to "hold" the peptides near the bilayer–water interface. In fact, in the case of an in-plane orientation of the peptide, hydrophobic amino acids can be more than 10 Å away

from the center of the bilayer [46]. Positively charged side chains such as the ones of lysines and arginines are also fundamental players in the partitioning of the peptides at bilayer–water interfaces. For instance, as amphipathic peptides are drawn to the hydrophobic interstices of bilayers, the long side chain of lysine can remediate unfavorable interactions with the hydrophobic core by snorkeling its charged amino end at the interface [47].

A number of interesting features have been described for histidine-containing peptides. Being around physiological pH, the pK_a of the histidine side chain depends on the local environment and cannot be easily predicted. Therefore the protonation state and charge of this side chain are not always known for a given peptide. pK_a values have been reported to be about 6 for several membrane-bound peptides studied by NMR [43,48] and UV [49]. Recently, the structure of SDS-bound Hb-33–61 indicated that the pK_a's of its histidine side chains were on the order of 7.7 to 7.8 [50], which is significantly high but understandable due to possible micelle–peptide interactions. Small changes of the vicinal pH may have large effects on the amphipathicity and activity of histidine-containing ACAPs. As a way of example, using histidines as pH-sensitive switches, the delivery of DNA into cells using synthetic, histidine-rich, pH-sensitive LAH4 peptides was brilliantly achieved [51]. Clavanins, antimicrobial peptides from chordates, which also have a high content of histidines but a cationic character (pI of 8.75) lower than piscidin, have pH-dependent antimicrobial activity featuring low activity at physiological pH, presumably due to the deprotonation of the histidines and a significant loss of cationic character [2]. With respect to piscidins, the presence of multiple histidines may contribute to their positive charge under physiological conditions, depending on the pK_a's of these residues in their given environment.

Earlier functional studies indicate that piscidins are highly potent antimicrobial peptides. Silphaduang and Noga tested the antimicrobial activity of piscidins 1, 2, and 3 and reported that they exist as a mixture of amidated and non-amidated peptides while Lauth et al. studied the activity of synthetic amidated piscidin 2 against numerous microorganisms. According to these studies, piscidin 1 (FFHHIFRGIVHVGK-TIHRLVTG-COO^-/NH_2, p1-COO^-/NH_2) is the most active piscidin, while the least active of the three is piscidin 3 (FIHHIFRGIVHAGRSIGRFLTG-COO^-/NH_2, p3-COO^-/NH_2), which compared to piscidin 1, lacks a histidine at position 17-. The MICs of piscidin 1 for most bacteria tested (<10 μM) [1,2] are in the range of the most effective ACAPs (0.1–10 μM) [20]. Piscidin 3 is significantly less hemolytic (~5% at 100 μg/mL) than piscidins 2 and 3 (~20% hemolytic at 20 μg/mL and ~95% at 100 μg/mL). From a structural standpoint, based on their amino-acid structures and functional roles, it was hypothesized early that piscidins adopt an amphipathic α-helical structure [1]. In fact, piscidin 2 was found to be α-helical in a 50/50 (v/v) mixture of TFE and phosphate buffer at pH 7.25. More recently, we used solid-state NMR to study piscidins 1 and 3. We characterized piscidin 1 as being α-helical in the presence of hydrated lipid bilayers while amidated piscidins 1 and 3 were shown to lie in the plane of the lipid bilayer [52].

Here, we compare amidated and non-amidated piscidins 1 and 3 in terms of their secondary structure, dynamics, and topology with respect to the lipid bilayer. The function is assessed by their individual antimicrobial activity. Hemolytic assays, which are traditionally used to determine the toxicity of antimicrobials against mammalian cells, were carried out, as well. To probe local structure and dynamics, we took advantage of solid-state NMR, which can be performed on site-specific isotopically-labeled peptides [37,53–57]. We employed complementary solid-state NMR orientational restraints to probe the structure and topology of piscidins in the membrane-bound state. Specifically, PISEMA (Polarization Inversion Spin Exchange at the Magic Angle) [58–61] was performed on oriented samples. A number of circular dichroism (CD) experiments were also carried out and interpreted qualitatively to aid the solid-state NMR work. Our investigation of amidated and non-amidated piscidins 1 and 3 is an attempt to characterize similarities and differences between these peptides to better understand structure–function relationships, and more particularly, the structural motifs involved in biological activity and functional diversity among variants. Since motions in ACAPs may be correlated to their ability to perturb lipid membranes and thereby define their mechanism(s) of action, we have incorporated dynamic information from solid-state NMR to our structural and functional studies. More detailed structural knowledge of ACAPs such as piscidins could help future selection and design of peptides which could have increased antimicrobial activity and reduced toxicity [4,18–21,34,62–64].

2. Materials and methods

2.1. Materials

All isotopically labeled peptides used for the structural studies (CD and solid-state NMR) were synthesized using Fmoc chemistry and solid phase peptide synthesis at United Biochemical Research (Seattle, WA). Following in house protection (Pacific Lutheran University) using well-established protocols [65–67], isotopically labeled amino acids (Cambridge Isotope Laboratories, Andover, MA) were incorporated in peptides as appropriate for the NMR studies. After synthesis and cleavage from the resin, peptides were purified using a Waters HPLC system and a Terra C18 column. The method consisted in a 25 min gradient of acetonitrile/water with 0.1% TFA. Peptides eluted at an acetonitrile concentration of approximately 30%. Purity was confirmed by mass spectroscopy. These peptides were also utilized for the antimicrobial and hemolytic assays to the exception of the amidated and non-amidated piscidin 1 used in antimicrobial assays, both of which were obtained from the University of Texas Southwestern Medical Center (UTSW) where their purity was determined using HPLC. Lipids were obtained from Avanti Polar Lipids (Alabaster, AL). Solvents (acetonitrile, chloroform, HPLC grade water, methanol, 2,2,2-trifluoroacetic acid, 2,2,2-trifluoroethanol) originated from Fisher Scientific (Pittsburgh, PA).

2.2. Antimicrobial assays

Bacterial strains used in this study were as follows: *Proteus vulgaris* , ATCC 13315; *Staphylococcus aureus*, ATCC 25923; *Bacillus cereus*, ATCC 25923;

Escherichia coli, ATCC 25922. The antimicrobial activity of amidated and non-amidated piscidins 1 and 3 was determined using a modified liquid growth assay described previously [2]. Briefly, logarithmic phase bacterial cultures were diluted 1 in 1000 in growth media (Todd Hewitt Broth). Synthetic amidated or non-amidated piscidins 1 and 3 dissolved in sterile double distilled water were added to 85 μL of diluted bacteria to yield final peptide concentrations of 0, 2, 10, 20 and 30 μM. Absorbance at 600 nm was measured using a microplate reader (μQuant Biotek Instruments) before and after overnight. MICs were reported as a range bracketed by the highest peptide concentration allowing unperturbed bacterial growth and the lowest peptide concentration leading to maximum bacterial death.

2.3. Hemolytic assays

Hemolytic assays were performed as described previously [68]. Succinctly, a defined concentration of peptides was added to a 5% suspension of freshly drawn human erythrocytes, which had been washed twice in phosphate-buffered saline. The suspension was incubated at 37 °C for 30 min prior to centrifugation at 10,000×*g* for 10 min. The absorbance at 400 nm was measured. Complete hemolysis was obtained by adding 0.2% Triton X-100 in place of the peptides.

2.4. Circular dichroism

Lipid films were prepared in a round bottom flask by dissolving phosphocholine (PC) and phosphoglycerate (PG) in a 3:1 molar ratio in chloroform. POPC (1-Palmitoyl-2-Oleoyl-*sn*-glycero-3-phosphocholine and POPG (1-Palmitoyl-2-Oleoyl-*sn*-glycero-3-phosphoglycerate) were used for piscidin 1 while DMPC (1,2-dimyristoyl-*sn*-glycero-3-phosphocholine) and DMPG (1,2-dimyristoyl-*sn*-glycero-3-phosphoglycerate) were used for piscidin 3. After rotary evaporation to form a thin layer around the walls of the round bottom flask, samples were dried under high vacuum. The lipid films were then hydrated with a phosphate buffer at pH 7.0 and incubated for 40 min in a water bath at 40 °C. The lipid suspensions were extruded at 35–40 °C, above the phase transition T_m of the lipids, using an Avanti Polar Lipid Mini Extruder and filters with 200 nm pores to obtain Large Unilamelar Vesicles (LUVs). Peptide solutions of 100 μM were prepared by dissolving the peptide in phosphate buffer at pH 7.0. The peptide and lipids were mixed to yield a 1:30 peptide to lipid ratio and a final peptide concentration of about 30 μM. CD spectra were obtained on a Jasco 720 CD Spectrometer at the University of Washington Department of Chemistry. Parameters were as follows: temperature of 25 °C, 1 mm quartz cuvette, scanning range from 270 to 195 nm, scanning speed of 100 nm/min, and 2 nm bandwidth. A total of 15 scans were accumulated. Following background subtraction, the ellipticity θ in millidegrees was displayed as a function of the wavelength in nanometers.

2.5. Preparation of samples for solid-state NMR

Oriented samples were prepared by drying lipid films of DMPC and DMPG containing 10 to 12 mg of peptide. The molar peptide to lipid ratio for oriented samples was 1:20 and the DMPC to DMPG molar ratio was 3:1 unless otherwise indicated. The peptide–lipid films and a 20 mL phosphate buffer solution (NaH_2PO_4/Na_2HPO_4, pH 6) were both pre-warmed to about 40 °C and mixed. Following swirling to allow for complete suspension, the binding of the peptide to the lipid was allowed to occur overnight after which the samples were centrifuged at 46,000×*g* for 3.0 h at 4 °C. Following centrifugation, the pellet was spread on about 50 thin glass slides (dimensions $5.7\times12\times0.03$ mm^3 from Matsunami Trading Co., Japan). Thicker glass slides (dimensions $5.7\times12.0\times0.07$ mm^3 from Paul Marienfeld GmbH and Co., Germany) were used for the ^{15}N–V_{20} p1-COO^- sample. After equilibrium was reached in a chamber at a relative humidity greater than 90% in the presence of a saturated solution of K_2SO_4, buffer was added to the slides at a ratio of 1 μL of buffer per 1 mg of peptide/lipid mixture. Next, the slides were stacked and inserted into glass cells (internal dimensions $6\times20\times4$ mm^3, Vitrocom Inc., NJ). These cells, which were sealed with beeswax to preserve hydration, were incubated at 43 °C until the samples appeared clear and homogeneously hydrated.

2.6. Solid-state NMR experiments

^{31}P solid-state NMR spectra were collected on the 500 WB Varian Unity+ NMR spectrometer at the Environmental Molecular Sciences Laboratory (EMSL, Richland, WA). Typical experimental parameters included a resonance frequency of 202.49 MHz, a 4 μs 90° pulse on ^{31}P and ^1H decoupling. The temperature was 39 °C. One hundred twenty scans were acquired with a recycle delay of 3 s. The spectra were referenced to an 85% solution of H_3PO_4.

Standard [69] and low electric-field (E-field) flat coil $^{15}N/^1H$ probes (Gor'kov, P. L. et al., unpublished data) were used to collect ^{15}N chemical shifts and $^{15}N/^1H$ dipolar coupling information from oriented samples. The low-E probes built at the National High Magnetic Field Laboratory (NHMFL, Tallahassee, FL) feature variable temperature capability and a circuit with an efficient sample coil that maintains a homogeneous excitation radio-frequency field over the sample volume while preventing damaging overheating of the biological sample subjected to repetitive high power radio-frequency pulsing. The combined use of low-E field probes and the use of well-sealed samples allowed for the preservation of sample authenticity during the long and demanding PISEMA experiment. Another feature of the NHMFL probes used here is the option to easily switch between vertical and horizontal coil assemblies.

^{15}N cross-polarization experiments were performed at a resonance frequency of 50.69 MHz on the EMSL 500 WB Varian Unity+ NMR spectrometer. Experimental parameters included a temperature of 39 °C, a contact time of 0.8 ms, a cross-polarization field of about 48 kHz, a decoupling field of 65 kHz, and a recycle delay of 6 s.

PISEMA experiments were performed on the 600 MHz WB Bruker Avance ×3 NMR spectrometer at the NHMFL. Experimental parameters on the 600 MHz instrument were as follows: temperature of 40±0.1 °C, ^{15}N resonance frequency of 60.83 MHz, 24–48 t_1 increments with 256–1024 transients each, recycle delay of 4–6 s, B_1 ^1H decoupling field of ~60 kHz, and B_1 cross-polarization field of ~45 kHz. The dipolar axis was adjusted to account for the scaling factor of 0.81 arising from the application of phase-alternated Lee–Goldburg homonuclear decoupling [58,70]. ^{15}N chemical shifts (CS) were referenced to a saturated solution of $^{15}NH_4NO_3$ which resonates at +22.3 ppm with respect to liquid NH_3.

3. Results

3.1. Antimicrobial assays

Using amidated and non-amidated piscidins 1 and 3 (p1-NH_2/COO^- and p3-NH_2/COO^-), we investigated the functional significance of amidation and variations in amino acid content. Antimicrobial activity against two representative Gram-positive bacteria, *Staphylococcus aureus* and *Bacillus cereus,* and two Gram-negative bacteria, *Escherichia coli* and *Proteus vulgaris* was determined. The results, which are the average of at least two independent experiments, are summarized in Table 1. Within the accuracy of these results, amidation did not affect the MIC ranges. However, piscidin 1 and 3 performed differently on all bacteria except *S. aureus* and *P. vulgaris*. The MIC range for *S. aureus* was 0–2 μM for both amidated and non-amidated piscidins 1 and 3. In the case of *B. cereus*, the MIC range was 0–2 μM for p1-NH_2 and p1-COO^- while it was 2–10 μM for p3-NH_2 and p3-COO^-. p1-NH_2 and p1-COO^- were somewhat less potent against the Gram-negative bacteria. Their MIC against *E. coli* and *P. vulgaris* ranged from 2 to 10 μM. The MIC of piscidin 3 against *E. Coli* was greater than the one for gram-positive bacteria, as well, and reached a range of 10–20 μM. The MIC range of piscidin 3 against *P. vulgaris* was identical to the one against *B. cereus*, i.e., 2–10 μM.

3.2. Hemolytic assays

Similarly to the antimicrobial assays, we used amidated and non-amidated piscidins 1 and 3 to determine if the amidation and specific amino acid sequence of piscidin affect its hemolytic effects. Fig. 1 shows the percent hemolysis obtained at a peptide concentration of 100 μg/mL. Blood originating from two different human subjects was used and three independent assays were performed on each source of blood. p1-NH_2 and p1-COO^- yielded similar results, i.e., about 73±8 and 78±11% hemolysis, respectively. p3-NH_2 was next in strength with about 50±11% hemolysis. p3-COO^- with a percent hemolysis of about 15±2 was the least hemolytic of the piscidins tested.

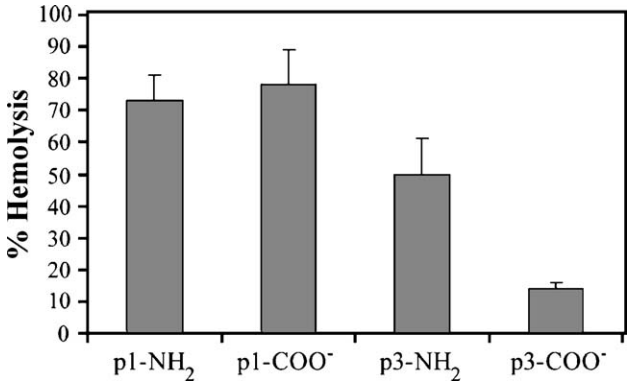

Fig. 1. Percent hemolysis for p1-NH_2, p1-COO^-, p3-NH_2, and p3-COO^-. The assays were performed using two different sources of human red blood cells. The results from three independent experiments for each source of blood were averaged and plotted here.

3.3. Circular dichroism

Since very small amounts of peptide are needed for CD experiments, we used this technique to assess the global secondary structure of amidated and non-amidated piscidins 1 and 3 under various sample conditions. This investigation was performed in parallel with the solid-state NMR experiments, which yielded site-specific, local information about secondary structure. Fig. 2 shows the appearance of secondary structure in amidated and non-amidated piscidins 1 and 3 upon exposure to 1:3 PC/PG LUVs at pH 7. As shown in Fig. 2, intense negative bands around 222 and 208 nm are observed indicating that p1-NH_2, p1-COO^-, p3-NH_2, and p3-COO^- adopt an α-helical conformation when the peptide to lipid ratio is 1:30. p3-NH_2 appears to have the highest helical content. The peptides behaved similarly at pH 5. α-helicity was observed whether a mixture of POPC/POPG or DMPC/DMPG was used (data not shown).

4. Solid-state NMR

4.1. ^{31}P and ^{15}N solid-state NMR on oriented samples

Oriented samples containing site-specific isotopically labeled amidated and non-amidated piscidins 1 and 3 were used to study peptide structure and dynamics. The alignment of the bilayers was checked by ^{31}P solid-state NMR, which takes advantage of the high natural abundance of ^{31}P nuclei present in the headgroups of phospholipid bilayers to obtain ^{31}P chemical shift spectra in a matter of minutes. The ^{31}P chemical shift was used to characterize the organization and macroscopic phases of the bilayers and determine the level of alignment in oriented samples. ^{15}N oriented chemical shifts were used to investigate the topology of the labeled peptides in hydrated lipid bilayers. While ^{31}P and ^{15}N chemical shift spectra were collected for each of the four piscidins, a representative subset of spectra is displayed and interpreted here. Fig. 3 shows the ^{31}P spectrum obtained for fully hydrated 3:1 DMPC/DMPG lipid bilayers containing p1-COO^- in a 1:50 peptide to lipid ratio while Fig. 4 displays the ^{15}N spectrum of ^{15}N-L_{20} p3-NH_2 interacting with fully hydrated 3:1 DMPC/DMPG in a 1:20 peptide to lipid ratio.

Multiple factors including molecular motions and uniform macroscopic alignment of the samples can be used to explain the sharp chemical shift resonances observed in Figs. 3 and 4. Chemical shift nuclear spin interactions, which dominate ^{31}P

Table 1
Antimicrobial activity of piscidins 1 and 3 against different microorganisms

Bacteria	ATCC #	MIC (μM)			
		p1-NH_2	p1-COO^-	p3-NH_2	p3-COO^-
Gram-Positive Bacteria					
Staphylococcus aureus	ATCC 25923	0–2	0–2	0–2	0–2
Bacillus cereus	ATCC 25923	0–2	0–2	2–10	2–10
Gram-Negative Bacteria					
Escherichia coli	ATCC 25922	2–10	2–10	10–20	10–20
Proteus vulgaris	ATCC 13315	2–10	2–10	2–10	2–10

ATCC #: American Type Culture Collection number; MIC: Minimum Inhibitory Concentration; p1: piscidin 1; p3: piscidin 3, COO^-: free carboxyl end; NH_2: carboxyamidated end.

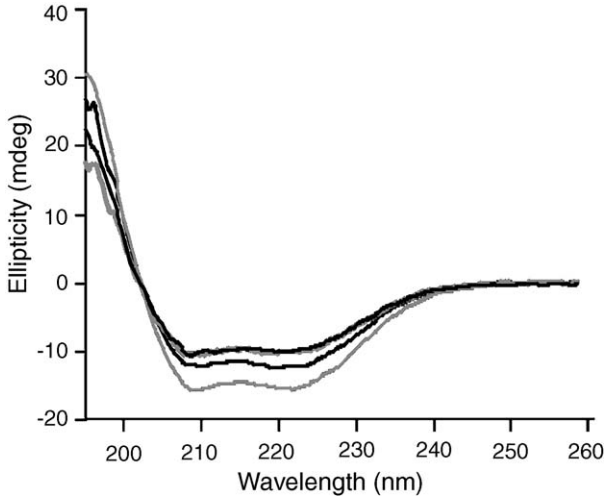

Fig. 2. Circular Dichroism. The ellipticity (mdeg) is displayed as a function of the wavelength (nm) as follows, from top to bottom where the curves start at 195 nm: p3-NH_2 (gray line), p1-NH_2 (black line), p3-COO^- (black line) and p1-COO^- (gray line) in 3:1 PC/PG at pH 7. The plots for p1-COO^- and p3-COO^- overlap above 200 nm.

and ^{15}N (spin ½) spectra obtained under ^{1}H decoupling, are anisotropic due their angular dependence with respect to the magnetic field B_0. More specifically, the chemical shift anisotropy (CSA) is due to the anisotropy of the electron density around the observed nuclei [71]. In unoriented samples containing molecules oriented randomly with respect to B_0, the CSA manifests itself by giving rise to broad chemical shift spectra for a specific nucleus due to the various orientations of the nuclear spins contributing to the spectrum. ^{31}P and ^{15}N anisotropic chemical shift spectra of static or immobilized molecules can give rise to "powder patterns" as wide as 200 ppm [71]. The three discontinuities observed in these spectra correspond to the three principal components (δ_{11}, δ_{22}, and δ_{33}, with $\delta_{11}>\delta_{22}>\delta_{33}$) of the 3×3 tensor used to represent the CSA [71]. Motions affect the spectra appearance and, in an extreme case, fast and isotropic motions in solution average the chemical shift interaction to an isotropic chemical shift. Phospholipid bilayers, which are of interest here, provide a good example to explore the effects of motions often observed in samples with solid-like properties [38,72,73]. Phospholipid molecules in hydrated bilayers do not undergo isotropic motions. Instead, they rotate fast around their long axis at temperatures above their phase transition, T_m. Consequently, motionally averaged ^{31}P chemical shift spectra of phospholipid bilayers in the fluid state are axially symmetric and characterized by two principal components, $\delta_{//}$ and $\delta_{\perp}$, both of which are shown in Fig. 3. $\delta_{//}$ corresponds to the chemical shift of lipid molecules oriented with their long axis parallel to B_0 while $\delta_{\perp}$ indicates the chemical shift of lipid molecules oriented perpendicular to B_0. Besides motions, the macroscopic orientations of molecules can also affect anisotropic chemical shift spectra. When all molecules are uniformly oriented with respect to a defined molecular axis such as a bilayer normal, the observed chemical shifts collapse to a single line representing the orientations of the observed nuclei and molecular axis with respect to B_0 [53,57,74,75]. Both spectra shown in Figs. 3 and 4 were obtained with the bilayer normal parallel to B_0. In this configuration, the bilayer normal is parallel to B_0 and the axis of motional averaging for the lipids. Hence, an intense ^{31}P chemical shift at $\delta_{//}$, as observed around 30 ppm in Fig. 3,

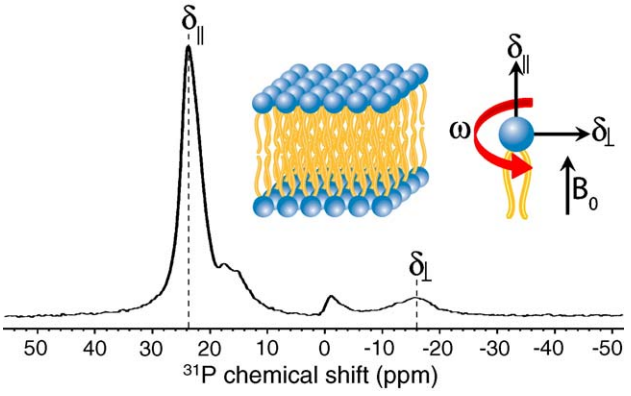

Fig. 3. ^{31}P solid-state NMR spectrum of fully hydrated oriented 3:1 DMPC/DMPG lipid bilayers containing p1-COO^- in a 1:50 peptide to lipid ratio at 40 °C. The sample was oriented so that the bilayer normal was parallel to the static magnetic field, B_0.

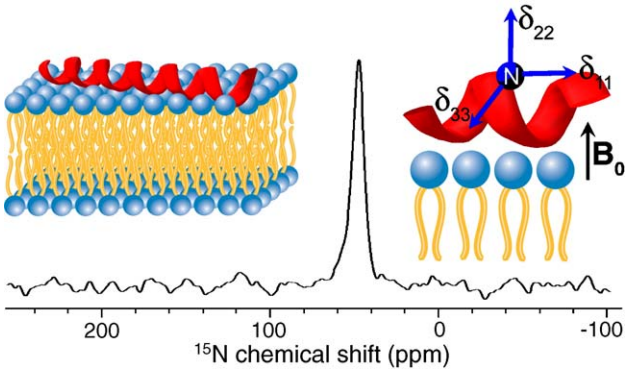

Fig. 4. ^{15}N solid-state NMR spectrum of L_{20}-p3-NH_2 in fully hydrated oriented 3:1 DMPC/DMPG lipid bilayers at 40 °C. 8616 scans were averaged. The sample was oriented so that the bilayer normal was parallel to the static magnetic field, B_0. The experiment was carried out on the EMSL 500 MHz Wide Bore spectrometer.

indicates that the lipid molecules are well aligned. A small amount of signal around −15 ppm ($\delta_{\perp}$) is indicative of unoriented bilayers.

Fig. 4 indicates that the amide ^{15}N anisotropic chemical shift resonance frequency for Leu_{20} in p3-NH_2 is 49.2 ppm (referenced to saturated $^{15}NH_4NO_3$). This chemical shift provides a powerful way to investigate the orientation of the peptide with respect to the molecular axis of orientation, i.e., the bilayer normal. Amide ^{15}N resonances are highly orientational dependent [53,54,57,74,75]. Since the secondary structure has already been assigned by REDOR for piscidin 1 [52] and piscidin 3 (D. J. Mitchell, B. S. Vollmar, and M. Cotten, unpublished data) and CD experiments for the four piscidins, ^{15}N backbone chemical shifts measured in oriented samples can be used to determine the orientation of the secondary structure element (i.e., helical axis) with respect to the bilayer normal and B_0. This interpretation is based on the principal component's values (δ_{11}, δ_{22}, and δ_{33}) of the amide ^{15}N chemical shift tensor and the orientation of this tensor with respect to the peptide plane and B_0. Advantageously, amide ^{15}N chemical shift tensors vary within a small range in polypeptides [76–87] with typical values for δ_{11}, δ_{22}, and δ_{33} around 200, 60, and 40 ppm, respectively. The orientation of the principal components with respect to the peptide plane is also well defined. Based on this approach, solid-state NMR has proven to be consistent in determining transmembrane and in-plane orientation of helices, and deciphering the disruptive effects of antimicrobial peptides on lipid membranes [37,42,53,54,57,75,88–104]. Here, based on CD and REDOR results indicating that piscidins 1 and 3 are α-helical in the presence of lipid bilayers, we interpret the observed ^{15}N chemical shifts around 50 ppm. As shown in Fig. 4, B_0 is oriented within the plane defined by δ_{22} and δ_{33}, indicating that the main axis of the α-helix is perpendicular to B_0 and the bilayer normal, and the peptide is oriented parallel to the bilayer surface. If the peptide had been transmembrane and parallel to the bilayer normal, the signal would have appeared around 180–200 ppm. Table 2 indicates that the amide ^{15}N oriented backbone chemical shifts for p1-NH_2, p1-COO^-, p3-NH_2, and p3-COO^- resonate around 45–66 ppm in 3:1 DMPC/DMPG. The positions of these

resonances and their sharpness indicate that each piscidin was very well aligned in these samples and the helical axis was oriented perpendicular to the bilayer normal [37,42,53,54,57,75,88–97]. To determine if the peptide could become transmembrane in longer-chain lipids, 3:1 POPC/POPG bilayers were also tested on piscidin 1. However, the chemical shift remained virtually unchanged indicating that hydrophobic mismatch between the 22-mer peptide and the shorter DMPC/DMPG chain was not the reason for the in-plane orientation of the peptide. We also changed the peptide to lipid ratio from 1:20 to 1:50 but this did not affect the chemical shift and linewidth indicating no signs of or changes in peptide aggregation states within that range of concentration (data not shown).

4.2. Studies of peptide backbone dynamics using ^{15}N solid-state NMR

To investigate peptide dynamics, we positioned oriented samples in the NMR probe so that the bilayer normal was perpendicular to B_0 (the so-called "90° orientation"). The ^{15}N NMR data collected on ^{15}N-V_{12} p1-COO^- at 20 and 40 °C are shown in Fig. 5. At 20 °C, the broad powder pattern indicates that below the phase transition of DMPC/DMPG (T_m of 23 °C), the ^{15}N chemical shift interactions are not averaged by fast, large amplitude motions and the peptide backbone is not moving fast on the NMR timescale [37,105]. As illustrated in the top part of Fig. 5, below T_m, the immobilized peptide experiences some level of orientation since it lies in the plane of the bilayers, but the helical axis of the numerous peptide molecules have different orientations with respect to the magnetic field resulting in a broad powder pattern. At 40 °C, above T_m, the broad powder pattern obtained at 20 °C is reduced to a narrow peak at 125 ppm. The sharpness of the resonance indicates that fast, large amplitude motions are present but they are not isotropic since the resonance frequency of the oriented chemical shift is significantly different from δ_{iso} (~100 ppm) [53,54,56,57,74,75]. Furthermore, this chemical shift is centered between δ_{11} and δ_{22}/δ_{33}, i.e., the edges of the static amide ^{15}N chemical shift powder pattern. As illustrated in Fig. 5, this result shows that, above T_m, the peptide experiences significant molecular motional averaging around an axis parallel to the bilayer normal and the motions are fast enough (i.e., on the order of a few kHz or more) to average out the singular orientations of the various peptide molecules in the plane of the bilayer. p1-NH_2, p1-COO^-, p3-NH_2, and p3-COO^- containing a ^{15}N-label at position 20 gave rise to similar results. Therefore, the four piscidins undergo motions around an axis parallel to the bilayer normal that are fast and large enough to average orientations in the plane of the bilayer [106,107].

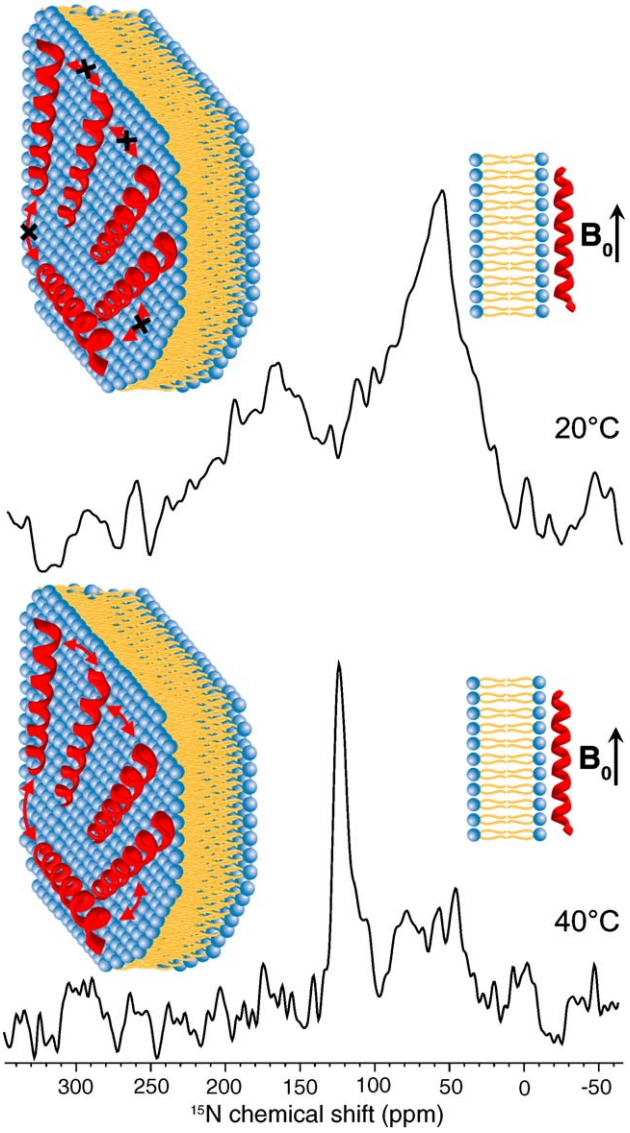

Fig. 5. ^{15}N solid-state NMR spectra of V_{12} p1-COO^- in fully hydrated oriented 3:1 DMPC/DMPG lipid bilayers at 20 (top) and 40 (bottom) °C. 2616 and 1154 scans were collected for the top and bottom spectra, respectively. The sample was oriented so that the bilayer normal was perpendicular to the static magnetic field, B_0. At 20 °C, below the phase transition temperature of the lipids, a static powder pattern is observed. At 40 °C, above the phase transition temperature of the lipids, the resonance at 125 ppm indicates that the peptide is undergoing fast motional averaging around an axis which is perpendicular to the magnetic field and parallel to the bilayer normal. Since the bilayer normal is perpendicular to the static magnetic field in this experiment, this resonance marks the upper edge of the motionally averaged powder pattern which would result from an unoriented version of this oriented sample. The spectra were recorded on the NHMFL 600 MHz Wide Bore spectrometer.

Table 2
^{15}N chemical shifts and ^{15}N–^{1}H dipolar couplings for piscidin 1 and piscidin 3

	^{15}N oriented chemical shifts[a]	^{15}N–^{1}H
	ppm	kHz
^{15}N–F_6 p1-COO^-	66.1±0.2	7.1±0.3
^{15}N–V_{10} p1-COO^-	57.1±0.2	8.3±0.3
^{15}N–V_{12} p1-COO^-	50.1±0.2	7.2±0.3
^{15}N–V_{20} p1-COO^-	50.7±0.2	8.4±0.3
^{15}N–V_{20} p1-NH_2	50.2±0.2	8.1±0.3
^{15}N–L_{20} p3-COO^-	46.7±0.2	8.9±0.3
^{15}N–L_{20} p3-NH_2	49.2±0.2	9.2±0.3

p1: piscidin 1; p3: piscidin 3, COO^-: free carboxyl end; NH_2: carboxyamidated end.

[a] Referenced to $^{15}NH_4NO_3$, which resonates at 22.3 ppm when referenced to $^{15}NH_3$.

4.3. PISEMA

In addition to providing information about the orientation of the peptide with respect to the bilayer normal, oriented samples can be used to characterize the peptide secondary structure. Indeed, if enough solid-state NMR orientational restraints such as ^{15}N chemical shifts and $^{15}N/^{1}H$ dipolar couplings are collected, they can be used to fully describe the high resolution backbone structure of membrane peptides and proteins [37,53,57,91,108,109]. 2-D PISEMA [53,58,70] experiments performed on oriented samples yield a ^{15}N chemical shift and a $^{15}N–^{1}H$ dipolar coupling for every peptide plane investigated. PISA (Polarity Index Slant Angle) wheel patterns observed in PISEMA spectra from helical segments can be analyzed to yield the tilt, polarity (rotation of the helix around its helical axis), and high-resolution structure of these stretches [57,92,108–110]. The center of the wheel relates to the tilt while indexing the signals on the wheels provides the polarity of the wheel. High-resolution PISEMA data sets were obtained for several backbone sites of piscidins in the presence of fully hydrated 3:1 DMPC/DMPG bilayers at a peptide to lipid ratio of 1:20 and a pH of 6. The data were collected above the phase transition of the lipids. The positions investigated were as follows: $^{15}N–F_6$, $^{15}N–V_{10}$, $^{15}N–V_{12}$, and $^{15}N–V_{20}$ in non-amidated piscidin 1, $^{15}N–V_{20}$ in amidated piscidin-1, and $^{15}N–L_{20}$ in amidated and non-amidated piscidin 3. Fig. 6 provides a comparison of p1-NH_2, p1-COO^-, p3-NH_2, and p3-COO^- at position 20. The four peptides yielded high-resolution spectra. As a way of example, the linewidth at half-height for $^{15}N–V_{20}$ p1-NH_2 is 600 Hz in the $^{15}N–^{1}H$ dipolar coupling dimension. Overall, upon comparisons of the piscidin PISEMA with excellent spectra published for various membrane bound species [57,94,110–114], we conclude that very good sensitivity and sample orientation were achieved for the piscidin samples investigated here. The four piscidins give rise to very similar chemical shifts and dipolar couplings at position 20, which is very close the carboxyl end and site of amidation for p1-NH_2 and p3-NH_2. This result demonstrates that the four peptides adopt very similar orientations with respect to B_0 and the bilayer normal, and their tilt and polarity are very similar at that

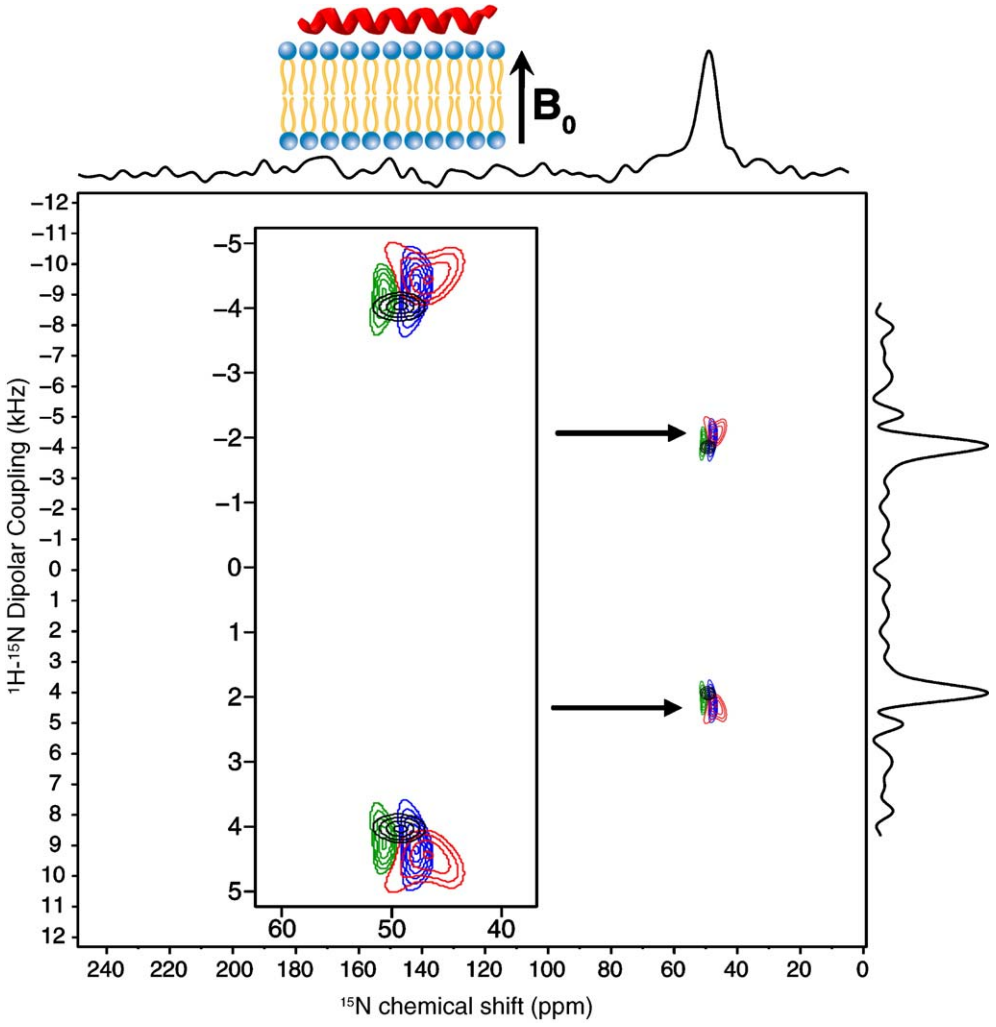

Fig. 6. 2-D PISEMA spectra for p1-NH2 (black), p1-COO^- (green), p3-NH2 (blue) and p3-COO^- (red) in fully hydrated oriented 3:1 DMPC/DMPG lipid bilayers at 40 °C. The sample was oriented so that the bilayer normal was parallel to the static magnetic field, B_0. The experiments were performed on the NHMFL 600 MHz Wide Bore spectrometer.

position. Table 2 summarizes the PISEMA results obtained for the different backbone positions investigated to date. Data do not vary very much at positions 10, 12, and 20. However, the $^{15}N–F_6$ chemical shift of p1-COO^- is significantly higher than the other chemical shifts explored along the peptide backbone. While the limited size of our data prevents us from concluding about the reasons underlying this result, several causes may be advanced to explain the spread of experimental chemical shifts values observed here. First, according to a simulation done by Wang et al. [110] for an ideal α-helix tilted at 90°, chemical shifts and dipolar couplings spread out to some extent. Second, Wang et al. indicate that multiple factors giving rise to deviations from predictions include the relative orientation of the ^{15}N chemical shift and $^{15}N–^{1}H$ dipolar interaction tensors, changes in tilt (τ) and polarity (ρ) along the length of the helix, differences in the ^{15}N chemical shift tensors, and local distortion(s) of the α-helix.

5. Discussion

The breath and depth of studies on α-helical antimicrobial amphipathic cationic peptides has brought new insights about the biological and physico-chemical properties of these peptides, which have the potential to be useful for the future selection and design of peptides with increased antimicrobial activity and reduced toxicity [4,18–21,34,62–64]. A number of questions remain outstanding. For instance, it has been challenging to establish a unifying view of relationships between structure and function, and the mechanisms of action of many ACAPs remain to be elucidated. Performing traditional structural/dynamic methods on physiologically relevant peptide–lipid samples is challenging, which explains that few ACAPs have been characterized at high-resolution in the presence of lipid bilayers. The structures of a few ACAPs exist in the PDB. Most of them were obtained in the presence of micelles or organic solvents [33]. While these studies have brought some insight about the structure of ACAPs, they do not necessarily allow us to appreciate subtle yet significant features of peptides binding lipid membranes and partitioning at the water–bilayer interface or inserting in the core of the membrane. Hence, it is important to study peptides and proteins active at membranes in the presence of the "most native-like bilayer environment", as recently reviewed by Opella and Marassi [57]. Moreover, since multiple mechanisms of action may exist for one given ACAP and several structures may be involved in the unfolding of each specific mechanism, it is also crucial to characterize these peptide structures and their topological features under stabilizing conditions.

The structural and functional studies presented here allow us to characterize a family of novel ACAPs from fish. Piscidins are particularly interesting systems due to numerous special features [1,2,7], which make them well-suited for structural and functional studies at the fundamental and applied levels. They are highly potent, highly cationic, histidine-rich, salt-tolerant, and they may naturally exist as a mixture of amidated and non-amidated peptides. Using two isoforms in their amidated and non-amidated forms, we have investigated the possible roles of sequence variations and carboxyamidation in the modulation of these peptides' function and structure. The antimicrobial assays performed here documents for the first time the individual antimicrobial activity of amidated versus non-amidated piscidins 1 and 3. Since the peptide threshold concentrations perturbing bacterial growth and leading to maximum antimicrobial effects were identical for amidated and non-amidated versions of a given isoform, we conclude that amidation did not affect the antimicrobial activity of these two peptides against the bacteria tested and at the peptide concentrations used here. Our results confirm earlier reports that piscidin 1 is more potent than piscidin 3 [1] and our MIC ranges on bacteria previously tested by Lauth et al. (i.e., *S. aureus* and *E. coli*) are comparable [2]. Difference in activity amongst isoforms of piscidins may be related to the ability of the peptides to interact with microbial membranes whose composition can vary greatly. For instance, Gram-negative bacteria have more complex cell walls than Gram-positive bacteria due to the presence of two lipid membranes and lipopolysaccharides on the outer surface of the outer membrane. Neutral PE (phosphatidylethanolamine), and anionic PG and DPG (diphosphatidylglycerol) are lipids commonly found in bacteria. Since the relative distribution of phospholipids between outer and inner leaflets of the bilayer is not well characterized, it is difficult to predict the nature of the lipid molecules first encountered by approaching antimicrobial peptides [34]. Both our relatively small data set on piscidins 1 and 3 and the extensive one presented by Lauth et al. [2] on amidated piscidin 2 suggest that piscidins may be more active against Gram-positive bacteria. Interestingly too, the lowest MIC of both piscidins 1 and 3 was obtained against Gram-positive *S. aureus* which, according to Ratledge [115], contains no PE in their cell membranes.

The hemolytic assays presented here confirm that piscidin 3 is less hemolytic than piscidin 1. While the hemolytic assays done by Silphaduang and Noga [1] did not distinguish between amidated and non-amidated peptides, their results also followed this trend. We also noticed that p3-COO^- appeared significantly less hemolytic than its amidated version. Due to the asymmetric transverse distribution of lipids in red blood cells, more neutral PC is present in the outer leaflet, which may reduce electrostatic interactions with ACAPs possibly explaining that, even though ACAPs, including piscidins, are usually hemolytic, 100% hemolysis often occurs at concentrations higher than the MICs. Other effects including hydrophobic forces may be at play, as well [26,116–118]. Ultimately, structural considerations help gain a better understanding of hemolytic and antimicrobial effects. Recently, Jin et al. [119] discussed findings showing that amphipathic structures, whether they are α-helices or β-sheets, were crucial for antimicrobial activity. Amphipathic α-helical peptides bind and destabilize PC containing membranes in agreement with their higher hemolytic effects compared to β-sheet peptides [116–118]. Notably here, our CD structural studies indicate that amidated and non-amidated piscidins 1 and 3 adopt α-helical structures in the presence of PC/PG LUVs.

Using solid-state NMR, we initiated the structural and dynamic study of amidated and non-amidated piscidins 1 and 3 in view of better understanding functional differences between isoforms and amidated versus non-amidated forms. Solid-state NMR offers several advantages for the study of membrane-

bound species. It is a powerful tool to investigate site-specific structure and dynamics. Based on amide ^{15}N oriented chemical shifts, we have demonstrated that the four piscidins adopt an orientation perpendicular to the bilayer normal indicating that amidation and variation in amino acid content do not affect the topology of piscidin. This orientation allows these amphipathic peptides to lie on the surface of the lipid bilayer. The amphipathic α-helical structure of piscidin is particularly well suited to partition at the water–bilayer interface based on the observation that the formation of secondary structure provides a strong contribution to the force driving the partitioning of peptides at interfaces [26,28,29,118,120]. Amidation is also an important factor since it relieves a negative charge at the carboxyl end and improves the binding energy. Both piscidins 1 and 3 have similar hydrophobic moments according to the scale developed by Whimley and White [45]. The protonation state of the histidine side chains is a factor which is also predicted to affect the binding of the peptide at the interface. Interestingly, neutral histidine side chains give rise to a lower hydrophobic moment for the helix [120], which would be expected to lower antimicrobial effects. The nature of the amino acids on the hydrophobic side of the helix is also determinant in influencing the ability of the peptide to bind bilayers. Both piscidins 1 and 3 contain phenylalanine, isoleucine, and leucine, which favor partitioning [45,120]. Overall, while these two isoforms have very similar sequences, there are some slight variations in the nature and distribution of the nonpolar and polar side chains around the helical wheel of piscidins 1 and 3 [1]. Added to the charge effects at the level of the histidine side chains, which may be protonated or deprotonated, and the carboxyl end, which may be amidated or not, these properties may combine to lead to the hemolytic and antimicrobial effects observed here.

In Fig. 3, results from ^{31}P NMR demonstrated that the oriented samples used in the present study were well aligned. A small shoulder on the right side of $\delta_{//}$, the aligned lipid signal, can be noticed. This feature is not unprecedented in PC/PG lipids containing antimicrobial peptides. Hallock et al. [42], who observed this effect in their investigation of pardaxin, attributed the phenomenon to a preferential binding of the cationic peptide to the negatively-charged PG headgroups as opposed to the neutral PC headgroups. The isotropic signal (i.e., around 0 ppm) in the ^{31}P spectrum shown in Fig. 3 may be due to lipids in an isotropic phase. Phosphate ions used in the hydrating buffer solution may contribute some ^{31}P isotropic signal, as well.

We also collected solid-state NMR orientational restraints using oriented samples containing amidated and non-amidated piscidins 1 and 3, as displayed in Figs. 4 and 6. High-quality PISEMA spectra were obtained for the four piscidins. They represent excellent results for peptides studied under physiologically relevant conditions. Linewidths for single crystals (i.e., close to perfect orientations) are on the order of 180 Hz [89]. Here, the narrow linewidths observed for the peptides in the presence of hydrated DMPC/DMPG bilayers (e.g., 600 Hz for p1-NH_2) indicates that excellent resolution can be achieved in complex mixtures of peptide, lipids, and water. The sensitivity and resolution achieved with these peptides is significant since experimental challenges exist for the detailed structural characterization of peptides with an in-plane bilayer orientation [57,108]. In fact, the resolution observed here would translate in a serious advantage if further structural work were performed on multiple labeled peptides [57,108,121]. Piscidins can now be added to the list of naturally occurring antimicrobial peptides such as magainin [122], pardaxin [42], melittin [40], LL-37 [123], cecropin [95], and aurein [124], which have been site-specifically labeled and structurally studied by solid-state NMR in an in-plane bilayer orientation. LH4 [43] and KL-14 [106,107] are synthetic peptides, which have also been studied in a similar fashion while lying in the plane of the bilayer. In the case of our study, the results from the 2-D PISEMA provide additional information compared to the 1-D ^{15}N solid-state experiments. Since amidated and non-amidated piscidins 1 and 3 have an overall α-helical structure, and the ^{15}N and ^{15}N–^{1}H dipolar couplings obtained from PISEMA vary little at position 20, the peptides are shown to adopt similar orientation, tilt, and polarity in hydrated DMPC/DMPG bilayers.

The structural and dynamic data presented here were obtained from samples in which the peptide to lipid ratios varied from 1:20 to 1:30 for the ^{15}N NMR and CD experiments, respectively. According to calculations performed by Blazyk et al. [68] for a peptide with a molecular weight of ~2000 and an MIC of 8 μg/mL, there is a real potential for a very large number of peptide molecules to interact with the surface of bacterial plasma membranes at peptide concentrations comparable to the MICs determined for piscidin. The authors indicate that their prediction remains meaningful even if not all of the peptide molecules reach the plasma membranes of the bacterial cells. On the basis of this prediction, the peptide concentrations used in the studies presented here are relevant to conditions under which the antimicrobial activity of piscidin is estimated to take place.

As demonstrated here for piscidin, the relatively small size of ACAPS can allow them to be highly mobile. Fast and large amplitude backbone motions in piscidins were detected in oriented samples using ^{15}N solid-state NMR (Fig. 5). More precisely, piscidin was found to experience global motional averaging around an axis parallel to the bilayer normal. Interestingly, this appears to be a situation in which both a well-defined structure and a planar orientation help the peptide achieve fast and large amplitude motions. Since these backbone motions stop below the phase transition of the lipids, a parallel can be established between the fluidity of the lipid bilayer and the motions of piscidin. The strong temperature dependence of these motions, especially around T_m, suggests that motions are not librational in nature but rather concerted global motions along the peptide backbone. This dynamics may have functional implications since it could provide a mechanism for the perturbation of cell membranes. Furthermore, it can be used to provide insight into the aggregation state of the peptide. In light of ^{15}N and ^{2}H solid-state NMR studies of KL-14, Bechinger and coworkers proposed that aggregation was not taking place [106]. Repulsion between highly positively charged peptides was proposed to be at play and favor the monomeric state over oligomerization. We propose that this reasoning also applies to piscidin under the experimental conditions tested here.

6. Conclusion

Since piscidins naturally occur as a mixture of amidated and non-amidated peptides, they represent an interesting system to study the possible significance of amidation both at the structural and functional levels. Amidation did not affect the antimicrobial activity and the topology of the peptides. Overall, piscidin 1 was confirmed to be more antimicrobial and hemolytic than piscidin 3. Peptide motions proved to be modulated by the physical state of the lipids. No fundamental structural differences have been identified in these peptides at position 20, which is close to the site of amidation. However, focusing on the features shared by the four piscidins such as an in-plane bilayer orientation at pH 6 and fast, large amplitude backbone motions, we propose that these properties contribute to the strong antimicrobial activity and particular features of these peptides. The in-plane orientation of these α-helical amphipathic peptides, which partition at the water–bilayer interface, appears to optimize peptide–lipid interactions and it is consistent with the carpet and in-plane diffusion mechanisms [4,20–22,30–33,36–38]. Fast, large amplitude motions occurring in the plane of the bilayer above the phase transition of the lipids may contribute to the perturbation of lipid organization, which may facilitate the induction of cell death. In closing, excellent PISEMA data indicate the feasibility of obtaining the high-resolution structures [57,108,110,121] of amidated and non-amidated piscidins 1 and 3 so that differences in potency and toxicity can be better understood. This knowledge will not only benefit research on ACAPs and broad spectrum drugs but it will also provide insight about other species active at membranes including membrane proteins and fusion peptides.

Acknowledgments

We acknowledge support from Research Corporation and the Camille and Henry Dreyfus Foundation, and NIH (GM-64676 for Eduard Y. Chekmenev's funding). We are grateful for NMR time allocated at the Environmental Molecular Sciences Laboratory (EMSL), a national scientific user facility sponsored by the Department of Energy's Office of Biological and Environmental Research and located at Pacific Northwest National Laboratory, and the National High Magnetic Field Laboratory (NHMFL) supported by Cooperative Agreement (DMR-0084173) and the State of Florida. We particularly thank Dr. Cross (NHMFL) and Dr. Ford (EMSL).

References

[1] U. Silphaduang, E.J. Noga, Peptide antibiotics in mast cells of fish, Nature 414 (2001) 268–269.
[2] X. Lauth, H. Shike, J.C. Burns, M.E. Westerman, V.E. Ostland, J.M. Carlberg, J.C. Van Olst, V. Nizet, S.W. Taylor, C. Shimizu, P. Bulet, Discovery and characterization of two isoforms of moronecidin, a novel antimicrobial peptide from hybrid striped bass, J. Biol. Chem. 277 (2002) 5030–5039.
[3] T. Ganz, R.I. Lehrer, Antimicrobial peptides of vertebrates, Curr. Opin. Immunol. 10 (1998) 41–44.
[4] T. Ganz, R.I. Lehrer, Antibiotic peptides from higher eukaryotes: biology and applications, Mol. Med. Today 5 (1999) 292–297.
[5] D.A. Devine, R.E.W. Hancock, Cationic peptides: distribution and mechanisms of resistance, Curr. Pharm. Des. 8 (2002) 703–714.
[6] K. Brogden, M. Ackermann, P.J. McCray, B. Tack, Antimicrobial peptides in animals and their role in host defences, Int. J. Antimicrob. Agents 22 (2003) 465–478.
[7] E.J. Noga, U. Silphaduang, Piscidins: a novel family of peptide antibiotics from fish, Drug News Perspect. 16 (2003) 87–92.
[8] A. Patrzykat, S.E. Douglas, Gone gene fishing: how to catch novel marine antimicrobials, Trends Biotech. 21 (2003) 362–369.
[9] N. Iijima, N. Tanimoto, Y. Emoto, Y. Morita, K. Uematsu, T. Murakami, T. Nakai, Purification and characterization of three isoforms of chrysophsin, a novel antimicrobial peptide in the gills of the red sea bream, Chrysophrys major, Eur. J. Biochem. 270 (2003) 675–686.
[10] H. Shike, X. Lauth, M.E. Westerman, V.E. Ostland, J.M. Carlberg, J.C. Van Olst, C. Shimizu, P. Bulet, J.C. Burns, Bass hepcidin is a novel antimicrobial peptide induced by bacterial challenge, Eur. J. Biochem. 269 (2002) 2232–2237.
[11] G.A. Birkemo, T. Lüders, O. Andersen, I.F. Nes, J. Nissen-Meyer, Hipposin, a histone-derived antimicrobial peptide in Atlantic halibut (*Hippoglossus hippoglossus* L), Biochim. Biophys. Acta 1646 (2003) 207–215.
[12] C.B. Park, J.H. Lee, I.Y. Park, M.S. Kim, S.C. Kim, A novel antimicrobial peptide from the loach, *Misgurnus anguillicaudatus*, FEBS Lett. 411 (1997) 173–178.
[13] A.M. Cole, P. Weis, G. Diamond, Isolation and characterization of pleurocidin, an antimicrobial peptide in the skin secretions of winter flounder, J. Biol. Chem. (1997) 12008–12013.
[14] R.T. Syvitski, I. Burton, N.R. Mattatall, S.E. Douglas, D.L. Jakeman, Structural characterization of the antimicrobial peptide pleurocidin from winter flounder, Biochemistry 44 (2005) 7282–7293.
[15] Z. Oren, Y. Shai, A class of highly potent antibacterial peptides derived from pardaxin, a pore-forming peptide isolated from Moses sole fish *Pardachirus marmoratus*, Eur. J. Biochem. 237 (1996) 303–310.
[16] V. Chinchar, L. Bryan, U. Silphadaung, E. Noga, D. Wade, L. Rollins-Smith, Inactivation of viruses infecting ectothermic animals by amphibian and piscine antimicrobial peptides, Virology 323 (2004) 268–275.
[17] R.M. Epand, H.J. Vogel, Diversity of antimicrobial peptides and their mechanisms of action, Biochim. Biophys. Acta 1462 (1999) 11–28.
[18] W. van't Hof, E. Veerman, E. Helmerhorst, A.V. Nieuw, Antimicrobial peptides: properties and applicability, Biol. Chem. 382 (2001) 597–619.
[19] M. Zasloff, Antimicrobial peptides of multicellular organisms, Nature 415 (2002) 389–395.
[20] A. Koczulla, R. Bals, Antimicrobial peptides: current status and therapeutic potential, Drugs 63 (2003) 389–406.
[21] S.H. Marshall, G. Arenas, Antimicrobial peptides: a natural alternative to chemical antibiotics and a potential for applied biotechnology, J. Biotech. 6 (2003) 272–284.
[22] K. Brogden, Antimicrobial peptides: pore formers or metabolic inhibitors in bacteria, Nat. Rev., Microbiol. 3 (2005) 239–250.
[23] Y. Shai, From innate immunity to de-novo designed antimicrobial peptides, Curr. Pharm. Des. 66 (2002) 715–725.
[24] J.D. Lear, Z.R. Wasserman, W.F. DeGrado, Synthetic amphiphilic peptide models for protein ion channels, Science 240 (1988) 1177–1181.
[25] Y. Agawa, S. Lee, S. Ono, H. Aoyagi, M. Ohno, T. Taniguchi, K. Anzai, Y. Kirino, Interaction with phospholipid bilayers, ion channel formation, and antimicrobial activity of basic amphipathic alpha-helical model peptides of various chain lengths, J. Biol. Chem. 266 (1991) 20218–20222.
[26] M. Dathe, M. Schumann, T. Wieprecht, A. Winkler, M. Beyermann, E. Krause, K. Matsuzaki, O. Murase, M. Bienert, Peptide helicity and membrane surface charge modulate the balance of electrostatic and hydrophobic interactions with lipid bilayers and biological membranes, Biochemistry 35 (1996) 12612–12622.
[27] Y. Shai, Mechanism of the binding, insertion and destabilization of phospholipid bilayer membranes by alpha-helical antimicrobial and cell

non-selective membrane-lytic peptides, Biochim. Biophys. Acta 1462 (1999) 55–70.
[28] N. Sitaram, R. Nagaraj, Interaction of antimicrobial peptides with biological and model membranes: structural and charge requirements for activity, Biochim. Biophys. Acta 1462 (1999) 29–54.
[29] M. Dathe, H. Nikolenko, J. Meyer, M. Beyermann, M. Bienert, Optimization of the antimicrobial activity of magainin peptides by modification of charge, FEBS Lett. 501 (2001) 146–150.
[30] R.E.W. Hancock, A. Rozek, Role of membranes in the activities of antimicrobial cationic peptides, FEMS Microbiol. Lett. 206 (2002) 143–149.
[31] Y. Shai, Mode of action of membrane active antimicrobial peptides, Biopolymers 66 (2002) 236–248.
[32] P.M. Hwang, H.J. Vogel, Structure–function relationships of antimicrobial peptides, Biochem. Cell Biol. 76 (1998) 235–246.
[33] J.P. Powers, R.E. Hancock, The relationship between peptide structure and antibacterial activity, Peptides 24 (2003) 1681–1691.
[34] K. Lohner, S.E. Blondelle, Molecular mechanisms of membrane perturbation by antimicrobial peptides and the use of biophysical studies in the design of novel peptide antibiotics, Comb. Chem. High Throughput Screen. 8 (2005) 241–256.
[35] L.J.V. Piddock, Antibacterials—Mechanisms of action, Curr. Opin. Struct. Biol. 1 (1998) 502–508.
[36] H.W. Huang, Action of antimicrobial peptides: two-state model, Biochemistry 39 (2000) 8347–8352.
[37] B. Bechinger, The structure, dynamics and orientation of antimicrobial peptides in membranes by multidimensional solid-state NMR spectroscopy, Biochim. Biophys. Acta 1462 (1999) 157–183.
[38] B. Bechinger, Detergent-like properties of magainin antibiotic peptides: a 31P solid-state NMR spectroscopy study, Biochim. Biophys. Acta 1712 (2005) 101–108.
[39] R.E.W. Hancock, The bacterial outer membrane as a drug barrier, Trends Microbiol. 5 (1997) 37–42.
[40] R. Smith, F. Separovic, T.J. Milne, A. Whittaker, F.M. Bennett, B.A. Cornell, A. Makriyannis, Structure and orientation of the pore-forming peptide, melittin, in lipid bilayers, J. Mol. Biol. 241 (1994) 456–466.
[41] Y. Lam, S.R. Wassall, C.J. Morton, R. Smith, F. Separovic, Solid-state NMR structure determination of melittin in a lipid environment, Biophys. J. 81 (2001) 2752–2761.
[42] K.J. Hallock, D.K. Lee, J. Omnaas, H.I. Mosberg, A. Ramamoorthy, Membrane composition determines pardaxin's mechanism of lipid bilayer disruption, Biophys. J. 83 (2002) 1004–1013.
[43] B. Bechinger, Towards membrane protein design: pH-sensitive topology of histidine-containing polypeptides, J. Mol. Biol. 263 (1996) 768–775.
[44] G. von Heijne, Membrane proteins: from sequence to structure, Annu. Rev. Biophys. Biochem. Struct. 23 (1994) 167–192.
[45] W.C. Wimley, S.H. White, Experimentally determined hydrophobicity scale for proteins at membrane interfaces, Nat. Struct. Biol. 3 (1996) 842–848.
[46] K. Matsuzaki, O. Murase, H. Tokuda, S. Funakoshi, N. Fujii, K. Miyajima, Orientational and aggregational states of magainin 2 in phospholipid bilayers, Biochemistry 33 (1994) 3342–3349.
[47] V. Mishra, M. Palgunachari, J.P. Segrest, G. Anantharamaiah, Interactions of synthetic peptide analogs of the class A amphipathic helix with lipids. Evidence for the snorkel hypthesis, J. Biol. Chem. 269 (1994) 7185–7191.
[48] T.C. Vogt, B. Bechinger, The Interactions of histidine-containing amphipathic helical peptide antibiotics with lipid bilayers. The effects of charges and pH, J. Biol. Chem. 274 (1999) 29115–29121.
[49] A. Okada, T. Miura, H. Takeuchi, Protonation of histidine and histidine–tryptophan interaction in the activation of the M2 ion channel from influenza a virus, Biochemistry 40 (2001) 6053–6060.
[50] M.L. Sforça, A. Machado, R.C. Figueredo, S.J. Oyama, F.D. Silva, A. Miranda, S. Daffre, M.T. Miranda, A. Spisni, T.A. Pertinhez, The micelle-bound structure of an antimicrobial peptide derived from the alpha-chain of bovine hemoglobin isolated from the tick Boophilus microplus, Biochemistry 44 (2005) 6440–6451.
[51] A. Kichler, C. Leborgne, J. März, O. Danos, B. Bechinger, Histidine-rich amphipathic peptide antibiotics promote efficient delivery of DNA into mammalian cells, Proc. Nat. Acad. Sci. 100 (2003) 1564–1568.
[52] E.Y. Chekmenev, S.M. Jones, Y.N. Nikolayeva, B.S. Vollmar, T.J. Wagner, P.L. Gor'kov, W.W. Brey, M.N. Manion, K.C. Daugherty, M. Cotten, High-Field NMR Studies of Molecular Recognition and Structure–Function Relationships in Antimicrobial Piscidins at the Water–Lipid Bilayer Interface, J. Am. Chem. Soc. 128 (2006) 5308–5309.
[53] R. Fu, T.A. Cross, Solid-state NMR investigation of protein and polypeptide structure, Annu. Rev. Biophys. Biomol. Struct. 28 (1999) 235–268.
[54] B. Bechinger, Biophysical investigations of membrane perturbations by polypeptides using solid-state NMR spectroscopy, Mol. Membr. Biol. 17 (2000) 135–142.
[55] A. Drechsler, F. Separovic, Solid-state NMR structure determination, IUBMB Life 55 (2003) 515–523.
[56] B. Bechinger, C. Aisenbrey, P. Bertani, The alignment, structure and dynamics of membrane-associated polypeptides by solid-state NMR spectroscopy, Biochim. Biophys. Acta 1666 (2004) 190–204.
[57] S.J. Opella, F. Marassi, Structure determination of membrane proteins by NMR spectroscopy, Chem. Rev. 104 (2004) 3587–3606.
[58] C.H. Wu, A. Ramamoorthy, S.J. Opella, High-resolution heteronuclear dipolar solid-state NMR spectroscopy, J. Magn. Reson. A 109 (1994) 270–272.
[59] A. Ramamoorthy, Y. Wei, D.K. Lee, PISEMA solid-state NMR spectroscopy, Annu. Rep. NMR Spectrosc. 52 (2004) 1–52.
[60] D.K. Lee, T. Narasimhaswamy, A. Ramamoorthy, PITANSEMA, A low-Power PISEMA solid-state NMR experiment, Chem. Phys. Lett. 399 (2004) 359–362.
[61] K. Yamamoto, D.E. Lee, A. Ramamoorthy, Broadband-PISEMA solid-state NMR spectroscopy, Chem. Phys. Lett. 407 (2005) 289–293.
[62] N. Sitaram, R. Nagaraj, The therapeutic potential of host-defense antimicrobial peptides, Curr. Drug Targets. 3 (2002) 259–267.
[63] J. Bradshaw, Cationic antimicrobial peptides: issues for potential clinical use, BioDrugs 17 (2003) 233–240.
[64] Y.J. Gordon, E.G. Romanowski, A.M. McDermott, A review of antimicrobial peptides and their therapeutic potential as anti-infective drugs, Curr. Eye Res. 30 (2005) 505–515.
[65] L.A. Carpino, G.Y. Han, The 9-fluorenylmethoxycarbonyl amino-protecting group, J. Org. Chem. 37 (1972) 3404–3409.
[66] G.B. Fields, C.G. Fields, J. Petefish, H.E. Van Wart, T.A. Cross, Solid phase peptide synthesis and solid state NMR spectroscopy of [Ala_3–^{15}N] [Val_1] gramicidin A, Proc. Natl. Acad. Sci. U.S.A. 85 (1988) 1384–1388.
[67] C.G. Fields, G.B. Fields, R.L. Noble, T.A. Cross, Solid phase peptide synthesis of ^{15}N-gramicidins A, B, and C and high performance liquid chromatographic purification, Int. J. Pept. Protein Res. 33 (1989) 298–303.
[68] J. Blazyk, R. Wiegand, J. Klein, J. Hammer, R.M. Epand, R.F. Epand, W.L. Maloy, U.P. Kari, A novel linear amphipathic beta-sheet cationic antimicrobial peptide with enhanced selectivity for bacterial lipids, J. Biol. Chem. 276 (2001) 27899–27906.
[69] P.L. Gor'kov, E.Y. Chekmenev, R. Fu, J. Hu, T.A. Cross, M. Cotten, W. W. Brey, A large volume flat coil probe for oriented membrane proteins, J. Magn. Reson. 181 (2006) 9–20.
[70] Z.T. Gu, S.J. Opella, Three-dimensional 13C shift/1H–15N coupling/15N shift solid-state NMR correlation spectroscopy, J. Magn. Reson. 138 (1999) 193–198.
[71] D.M. Grant, Chemical shift tensors in Encyclopedia of Nuclear Magnetic Resonance, in: D.M. Grant (Ed.), J. Wiley, Chichester/New York, 1996, pp. 1298–1321.
[72] J. Seelig, 31P nuclear magnetic resonance and the head group structure of phospholipids in membranes, Biochim. Biophys. Acta 515 (1978) 105–140.
[73] M. Auger, Membrane structure and dynamics as viewed by solid-state NMR spectroscopy, Biophys. Chem. 68 (1997) 233–241.
[74] T.A. Cross, S.J. Opella, Solid-state NMR structural studies of peptides and proteins in membranes, Curr. Opin. Struct. Biol. 4 (1994) 574–581.
[75] B. Bechinger, L.M. Gierasch, M. Montal, M. Zasloff, S.J. Opella,

Orientations of helical peptides in membrane bilayers by solid state NMR spectroscopy, Solid State NMR 7 (1996) 185–191.
[76] G.S. Harbison, R.E. Jelinsky, R.E. Stark, D.A. Torchia, J. Herzfeld, R.G. Griffin, 15N chemical shift and 15N-13C dipolar tensors for the peptide bond in (1–13C)Glycyl(15N)Glycine hydrochloride monohydrate, J. Magn. Reson. 60 (1984) 79–82.
[77] C.J. Hartzell, M. Whitfield, T.G. Oas, G.P. Drobny, Determination of the nitrogen-15 and carbon-13 chemical shift tensors of L-[13C]alanyl-L-[15N]alanine from the dipole-coupled powder patterns, J. Am. Chem. Soc. 109 (1987) 5966–5969.
[78] C.J. Hartzell, T.K. Pratum, G.P. Drobny, Mutual orientation of three magnetic tensors in a polycrystalline dipeptide by dipole modulated 15N chemical shift spectroscopy, J. Chem. Phys. 87 (1987) 4314–4331.
[79] Q. Teng, T.A. Cross, The in situ determination of the 15N chemical-shift tensor orientation in a polypeptide, J. Magn. Reson. 85 (1989) 439–447.
[80] C. Wu, A. Ramamoorthy, L.M. Gierasch, S.J. Opella, Simultaneous characterization of the amide 1H chemical shift, 1H-15N dipolar, and 15N chemical shift interaction tensors in a peptide bond by three-dimensional solid-state NMR Spectroscopy, J. Am. Chem. Soc. 117 (1995) 6148–6149.
[81] D.K. Lee, R.J. Wittebort, A. Ramamoorthy, Characterization of 15N chemical shift and 1H-15N dipolar coupling interactions in a peptide bond of uniaxially oriented and polycrystalline samples by one-dimensional dipolar—Chemical shift solid-state NMR spectroscopy, J. Am. Chem. Soc. 120 (1998) 8868–8874.
[82] D.K. Lee, J.S. Santos, A. Ramamoorthy, Nitrogen-15 chemical shift anisotropy and 1H-15N dipolar coupling tensors associated with the phenylalanine residue in the solid-state, Chem. Phys. Lett. 309 (1999) 209–214.
[83] J.R. Brender, D.M. Taylor, A. Ramamoorthy, Orientation of amide-nitrogen-15 chemical shift tensors in peptides: a Quantum Chemical Study, J. Am. Chem. Soc. 123 (2001) 914–922.
[84] Y. Wei, D.K. Lee, A. Ramamoorthy, A two-dimensional magic angle decoupling and magic angle turning solid-state NMR method—An application to study chemical shift tensors from peptides that are non-selectively labeled with 15N isotope, J. Phys. Chem., B 104 (2001) 4752–4762.
[85] E.Y. Chekmenev, Q. Zhang, K.W. Waddell, M.S. Mashuta, R.J. Wittebort, 15N chemical shielding in glycyl tripeptides: measurement by solid-state NMR and correlation with X-ray structure, J. Am. Chem. Soc. 126 (2003) 379–384.
[86] A. Poon, J. Birn, A. Ramamoorthy, How does an amide-N-15 chemical shift tensor vary in peptides? J. Phys. Chem., B 108 (2004) 16577–16585.
[87] K.W. Waddell, E.Y. Chekmenev, R.J. Wittebort, Single-crystal studies of peptide prolyl and glycyl 15N shielding tensors, J. Am. Chem. Soc. 127 (2004) 9030–9035.
[88] R.R. Ketchem, W. Hu, T.A. Cross, High-resolution conformation of gramicidin a in a lipid bilayer by solid state NMR, Science 261 (1993) 1457–1460.
[89] A. Ramamoorthy, F. Marassi, M. Zasloff, S.J. Opella, Three-dimensional solid-state NMR spectroscopy of a peptide oriented in membrane bilayers, J. Biomol. NMR 6 (1995) 329–334.
[90] M. Cotten, X. Feng, T.A. Cross, Protein stability and conformational rearrangements in lipid bilayers: linear gramicidin, a model system, Biophys. J. 73 (1997) 614–623.
[91] S.J. Opella, NMR and membrane proteins, Nat. Struct. Biol. 4 (1997) 845–848.
[92] F. Marassi, S.J. Opella, NMR structural studies of membrane proteins, Curr. Opin. Struct. Biol. 8 (1998) 640–648.
[93] M. Cotten, R. Fu, T.A. Cross, Solid-state NMR and hydrogen–deuterium exchange in a bilayer-solubilized peptide: structural and mechanistic implications, Biophys. J. 76 (1999) 1179–1189.
[94] F.M. Marassi, C. Ma, H. Gratkowski, S.K. Straus, K. Strebel, M. Oblatt-Montal, M. Montal, S.J. Opella, Correlation of the structural and functional domains in the membrane protein Vpu from HIV-1, Proc. Natl. Acad. Sci. U. S. A. 96 (1999) 14336–14341.
[95] F. Marassi, S.J. Opella, P. Juvvadi, R.B. Merrifield, Orientation of cecropin A helices in phospholipid bilayers determined by solid-state NMR spectroscopy, Biophys. J. 77 (1999) 3152–3155.
[96] K. Mattila, R. Kinder, B. Bechinger, The alignment of a voltage-sensing peptide in dodecylphosphocholine micelles and in oriented lipid bilayers by nuclear magnetic resonance and molecular modeling, Biophys. J. 77 (1999) 2102–2113.
[97] U. Harzer, B. Bechinger, Alignment of lysine-anchored membrane peptides under conditions of hydrophobic mstmatch: a CD, 15N, 31P solid-state NMR spectroscopy investigation, Biochemistry 39 (2000) 13106–13114.
[98] K.J. Hallock, D.K. Lee, A. Ramamoorthy, MSI-78, an analogue of the magainin antimicrobial peptides, disrupts lipid bilayer structure via positive curvature strain, Biophys. J. (2003) 3052–3060.
[99] K.A. Henzler-Wildman, G.V. Martinez, M.F. Brown, A. Ramamoorthy, Perturbation of the hydrophobic core of lipid bilayers by the human antimicrobial peptide LL-37, Biochemistry 43 (2004) 8459–8469.
[100] F. Porcelli, B. Buck, D.K. Lee, K.J. Hallock, A. Ramamoorthy, G. Veglia, Structure and orientation of pardaxin determined by NMR experiments in model membranes, J. Biol. Chem. 279 (2004) 45815–45823.
[101] A. Mecke, D.K. Lee, A. Ramamoorthy, B.G. Orr, M.M.B. Holl, Membrane thinning due to antimicrobial peptide binding: an atomic force microscopy study of MSI-78 in lipid bilayers, Biophys. J. 99 (2005) 4043–4050.
[102] J.P.S. Powers, A. Tan, A. Ramamoorthy, R.E.W. Hancock, Solution structure and interaction of the antimicrobial polyphemusins with lipid membranes, Biochemistry 44 (2005) 15504–15513.
[103] S. Thennarasu, D. Lee, A. Tan, U. Prasad Kari, A. Ramamoorthy, Antimicrobial activity and membrane selective interactions of a synthetic lipopeptide MSI-843, Biochim Biophys Acta. (2005) 49–58.
[104] S. Thennarasu, D.K. Lee, A. Poon, K.E. Kawulka, J.C. Vederas, A. Ramamoorthy, Membrane permeabilization, orientation, and antimicrobial mechanism of subtilosin A, Chem. Phys. Lipids 137 (2005) 38–51.
[105] G.P. Drobny, J.R. Long, W.S. Shaw, M. Cotten, P.S. Stayton, Studies of the Structure and Dynamics of Proteins Adsorbed to Biomaterial Interface, in: D.M. Grant, R.K. Harris (Eds.), Encyclopedia of Nuclear Magnetic Resonance, Advances in NMR, Vol. 9, John Wiley & Sons, Ltd., Chichester/New York, 2002, pp. 458–468.
[106] C. Aisenbrey, B. Bechinger, Tilt and rotational pitch angle of membrane-inserted polypeptides from combined 15N and 2H solid-state NMR, Biochemistry 43 (2004) 10502–10512.
[107] C. Aisenbrey, B. Bechinger, Investigations of polypeptide rotational diffusion in aligned membranes by 2H and 15N solid-state NMR Spectroscopy, J. Am. Chem. Soc. 126 (2004) 16676–16683.
[108] S.J. Opella, A. Nevzorov, M.F. Meslesh, F. Marassi, Structure determination of membrane proteins by NMR spectroscopy, Biochem. Cell Biol. 80 (2002) 597–604.
[109] F.M. Marassi, S.J. Opella, Simultaneous assignment and structure determination of a membrane protein from NMR orientational restraints, Protein Sci. 12 (2003) 403–411.
[110] J. Wang, J. Denny, C. Tian, S. Kim, Y. Mo, F. Kovacs, Z. Song, K. Nishimura, Z. Gan, R. Fu, J.R. Quine, T.A. Cross, Imaging membrane protein helical wheels, J. Magn. Reson. 144 (2000) 162–167.
[111] Y. Kim, K. Valentine, S.J. Opella, S. Schendel, W.A. Cramer, Solid-state NMR studies of the membrane-bound closed state of the colicin E1 channel domain in lipid bilayers, Protein Sci. 7 (1998) 342–348.
[112] F.M. Marassi, J.J. Gesell, A.P. Valente, Y. Kim, M. Oblatt-Montal, M. Montal, S.J. Opella, Dilute spin-exchange assignment of solid-state NMR spectra of oriented proteins: acetylcholine M2 in bilayer, J. Biomol. NMR 14 (1999) 141–148.
[113] Z. Song, F.A. Kovacs, J. Wang, J.K. Denny, S.C. Shekar, J.R. Quine, T.A. Cross, Transmembrane domain of M2 protein from influenza A virus studied by solid-state (15)N polarization inversion spin exchange at magic angle NMR, Biophys. J. 79 (2000) 767–775.
[114] C. Tian, P.F. Gao, L.H. Pinto, R.A. Lamb, T.A. Cross, Initial structural and dynamic characterization of the M2 protein transmembrane and amphipathic helices in lipid bilayers, Protein Sci. 12 (2003) 2597–2605.
[115] C. Ratledge, S.G. Wilkinson, Microbial Lipids, vol. 2, Elsevier Science and Technology Books, 1988.

[116] E.T. Kaiser, F.J. Kezdy, Peptides with affinity for membranes, Annu. Rev. Biophys. Biophys. Chem. 16 (1987) 561–581.
[117] M. Dathe, T. Wieprecht, Structural features of helical antimicrobial peptides: their potential to modulate activity on model membranes and biological cells, Biochim. Biophys. Acta 1462 (1999) 71–87.
[118] T. Wieprecht, O. Apostolov, M. Beyermann, J. Seelig, Thermodynamics of the alpha–helix–coil transition of amphipathic peptides in a membrane environment: implications for the peptide–membrane binding equilibrium, J. Mol. Biol. 294 (1999) 785–794.
[119] Y. Jin, H. Mozsolits, J. Hammer, E. Zmuda, F. Zhu, Y. Zhang, M.I. Aguilar, J. Blazyk, Influence of tryptophan on lipid binding of linear amphipathic cationic antimicrobial peptides, Biochemistry 42 (2003) 9395–9405.
[120] S. Jaysinghe, K. Hristova, S.H. White, http://blanco.biomol.uci.edu/mpex, (2000).
[121] F.M. Marassi, A. Ramamoorthy, S.J. Opella, Complete resolution of the solid-state NMR spectrum of a uniformly 15N-labeled membrane protein in phospholipid bilayers, Proc. Natl. Acad. Sci. U. S. A. 94 (1997) 8551–8556.
[122] A. Ramamoorthy, L.M. Gierasch, S.J. Opella, Four-dimensional solid-state NMR experiment that correlates the chemical-shift and dipolar-coupling frequencies of two heteronuclei with the exchange of dilute-spin magnetization, J. Magn. Reson., B 109 (1995) 112–116.
[123] K.A. Henzler-Wildman, D.K. Lee, A. Ramamoorthy, Mechanism of lipid bilayer disruption by the human antimicrobial peptide, LL-37, Biochemistry 42 (2003) 6545–6558.
[124] M.S. Balla, J.H. Bowie, F. Separovic, Solid-state NMR study of antimicrobial peptides from Australian frogs in phospholipid membranes, Eur. Biophys. J. 33 (2004) 109–116.